Scientia Iranica F (2015) 22(3), 1346–1356

SCIENTIA
IRANICA

Sharif University of Technology
Scientia Iranica
Transactions F: Nanotechnology
www.scientiairanica.com

Experimental investigation of nano zero-valent iron mobility in porous media

M.R. Fadaei Tehrani[a,*], **A. Shamsai**[a] **and M. Vossughi**[b]

a. *Department of Civil Engineering, Sharif University of Technology, Tehran, P.O. Box 11365-11155, Iran.*
b. *Institute of Biotechnology and Environment (IBE), Department of Chemical Engineering, Sharif University of Technology, Tehran, Iran.*

Received 5 January 2015; received in revised form 13 April 2015; accepted 16 June 2015

KEYWORDS
Remediation;
Mobility;
Nano zero-valent iron;
nZVI;
Groundwater.

Abstract. In this study, the colloidal stability and mobility of Fe/Ni nano particles, concurrently synthesized and stabilized in the presence of starch (S-nZVI/Ni), were investigated. In particular, the influence of pore velocity (ranging from 7 to 85 m/d) and injected particle concentrations (0.3 and 3 g/l) was evaluated in a one-dimensional column. Experimental results exposed the fine mobility of the S-nZVI/Ni particles in porous materials. According to the breakthrough curves and mass recovery, the S-nZVI travel distance was limited to the range of 0.2 to 0.4 m for low pore velocities (5 to 7 m/d), and in the order of 10 m at higher velocities (> 50 m/d). Moreover, increasing pore velocity enhanced the mobility of S-nZVI. Results also proposed that the mobility of S-nZVI suspension in sand media should be lower than in glass beads media. The clogging phenomenon of the column and the pore pressure variations during the injection period were strongly affected by media type and injected particle concentration. Clogging, due to the deposition of particles, was observed, in particular, for 3 g/l nZVI suspension, low velocities and sand media. Finally, the results indicated that starch stabilized iron nano particles have the potential to become an effective reactive material for in-situ groundwater remediation.

1. Introduction

Contamination of groundwater with pollutants is a threat to the environment and human health, so, it is essential to remediate polluted aquifers. The remediation of groundwater resources has been a subject of interest for several decades. However, conventional remediation and treatment technologies, such as pump and treat, have shown limited effectiveness in reducing contamination, and are expensive [1]. Recently, in-situ techniques for remediation, such as Permeable Reactive Barriers (PRBs), have become promising alternatives to ex-situ methods, owing to their lower operating costs [2]. Nano zero-valent iron particles, nZVI, could be used as reducing agents in PRBs for removing a wide range of pollutants. They promise to be significantly more effective than granular iron; the reaction rates are 20 to 30 times faster, and the sorption capacity is much higher compared with the granular form [3].

The greater total surface area of nZVI particles, along with higher reactive site density, that are present on the surface of the particles, and/or the more reactive nature of the sites, are considered causative factors in the higher reactivity of nZVI [4]. Numerous studies have utilized iron nano particles for remedia-

---

[*] *Corresponding author. Tel.: +98 21 66164201; Fax: +98 21 66036005*
E-mail addresses: fadaei@mehr.sharif.edu (M.R. Fadaei Tehrani); Shamsai@sharif.edu (A. Shamsai); vosoughi@sharif.edu (M. Vossughi).

tion of various contaminants, like chlorinated organic compounds and metal ions [5], nitrate [6,7], carbon tetrachloride, benzoquinone [8], metalloids, such as arsenic [9,10], and organic compounds [11]. However, there are some challenges in exploiting nZVI-based remediation techniques, which have made it difficult to engineer its application for optimal performance or to assess its probable risk to human or ecological health.

Due to their small size, nano particles could be injected into an aquifer as colloidal suspension, and are expected to penetrate easily in porous materials in order to reach the plume of contaminants. Furthermore, they should have adequate mobility to transport away from the injection point. However, it has been indicated that bare nZVI is hardly mobile and stable in laboratory and field-scale studies [12-14]. Crucial points are stability against aggregation, mobility in subsurface environments and longevity under subsurface conditions [15]. Typically, nZVI mobility from the injection point must be in the order of 10 m or more for field applications [16]. Modification of surface properties has been proposed as the main approach to enhance the colloidal stability of nZVI aqueous dispersion, and, consequently, improved mobility in porous media. Natural and engineered polymers and anionic surfactants, as well as other organic coatings, have been identified as promising materials for improving the colloidal stability of nZVI [17].

So far, several researchers have synthesized various stable nZVI suspensions, and characterized the mobility properties of the particles in porous media [17-19]. Phenrat et al. prepared stable nZVI slurry using 5 to 40 nm sized Fe°/Fe-oxide nanoparticles, along with several different types of polyelectrolyte. According to their results, the order of effectiveness for the prevention of rapid aggregation and dispersion stabilization was PSS70K (83%) > PAP10K (82%) > PAP2.5K (72%) > CMC700K (52%) [20].

In this study, the mobility of bimetallic Fe/Ni nanoparticles in a one-dimensional column was experimented. First, a stable suspension of nZVI was synthesized and stabilized by starch on-site. Then, several series of column experiments were planned to evaluate the impact of pore water velocity and slurry concentration on nZVI mobility. Two types of porous material were used:

(a) Glass beads, as a typical transparent inert medium;

(b) Packed sand, as a typical aquifer material.

Finally, the experimental data were modeled using a classic one-dimensional Convection-Dispersion flow Equation (CDE) in combination with the Colloid Filtration Theory (CFT).

2. Materials and methods

2.1. Materials

Chemicals used in this study, including $FeCl_3.6H_2O$, $NaBH_4$ and HCl, were purchased from Merck (Germany). A Hach DR 5000 spectrophotometer was utilized to measure total and ferrous iron concentrations, according to Hach methods of 8008 and 8146. The iron nanoparticles were prepared just before the experiments in order to lessen their surface oxidation. nZVI particles were synthesized by gradually adding 0.15 M $NaBH_4$ solution, at a rate of 1 to 2 mL/min, to 0.1 M $FeCl_3.6H_2O$ aqueous solution containing 10% starch. This was performed at ambient temperature and the resulted suspension was vigorously stirred at 400 rpm, according to the methodology of He and Zhao [21]. During this reaction, sodium borohydride reduced ferric ions into black particles, according to the following reaction [22]:

$$4Fe^{3+}_{(aq)} + 3BH_4 + 9H_2O \rightarrow 4Fe^{\circ}_{(s)} \downarrow + 3H_2BO_3 + 12H^{+}_{(aq)} + 6H_{2(g)} \uparrow . \quad (1)$$

Experiments were performed in saturated porous media using a plexi-glass column with a length of 0.6 m and an inner diameter of 0.05 m (Figure 1). The column was packed wet and was fed a background electrolyte solution with a Heidolph peristaltic pump (multichannel flow rates from 0.5 to 320 mL/min) for at least 10 Pore Volumes (PV) for removing background turbidity and providing a uniform collector surface charge.

Two types of porous media were used in column experiments, including glass beads and sand whose properties are listed in Table 1. Glass bead grains were of a spherical shape and particle size ranging between 0.4×10^{-3} and 0.6×10^{-3} m, and sand grains were of a globular shape and particle size ranging between 0.4×10^{-3} and 0.6×10^{-3} m. The source reservoir of S-nZVI was sonicated with ultrasonic equipment (Media safe, UK, LTD) to minimize both aggregation and sedimentation during slurry injection. A permeable glass diffuser screen was used at the column inlet to provide a uniform distribution in the cross section. The pressure drop along the column during the experiment was continuously measured at the inlet, middle, and outlet of the column.

Prior to each test, the glass beads were soaked in a hydrogen peroxide solution (5%) for 10 hr to remove impurities, washed with de-ionized water and, finally, baked at 105°C for 24 hr [23]. Also, the sand was immersed overnight in concentrated hydrochloric acid, in order to remove the background iron oxides, rinsed with de-ionized water, and dried in an oven at a temperature of 105°C. In all experiments, the pH of the input water was adjusted to 7 ± 0.2.

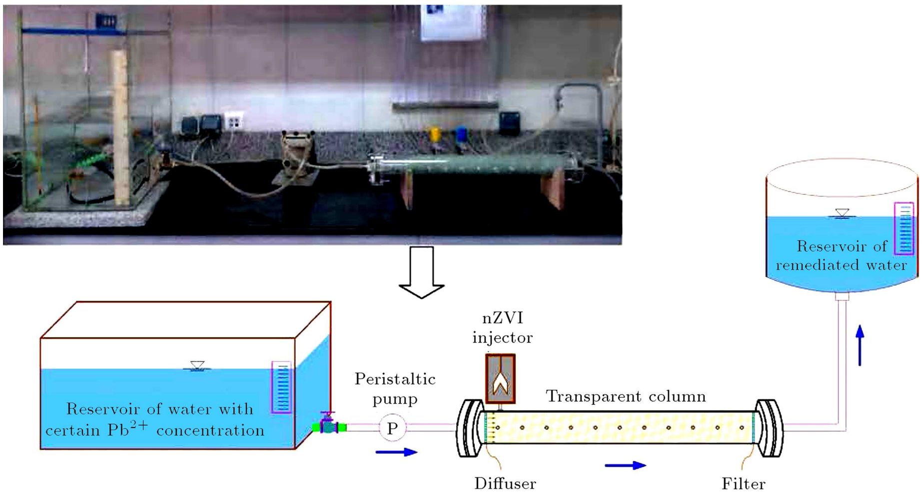

Figure 1. Picture and schematic of transparent column model.

Table 1. Properties of porous media used for column experiment.

Symbol	Porous media parameters	Value
L	Column length	60 cm
D	Column inner diameter	5 cm
	Collector diameter	
d_{50}	Glass beads	0.50 mm
	Sand	0.5 mm
	Collector porosity	
n	Glass beads	0.35
	Sand	0.31
	Collector pore volume	
PV	Glass beads	20 mL
	Sand	20 mL
	Collector density	
ρ_b	Glass beads	2.5 g/cm^3
	Sand	2.5 g/cm^3
	Collector dry bulk density	
ρ_b	Glass beads	1.7 g/cm^3
	Sand	1.7 g/cm^3
T	Temperature	20 ± 2

2.2. Methods

Colloid transportation in column experiments was modeled using a Classic Filtration Theory (CFT) [24]:

$$\frac{\partial C}{\partial t} = D\frac{\partial^2 C}{\partial x^2} - v\frac{\partial C}{\partial x} - K_{\text{att}}C, \tag{2}$$

where C is the nZVI concentration in the aqueous phase (M/L^3), D is the hydrodynamic dispersion coefficient (L^2/T), v is the pore velocity (L/T), t is time (T), and K_{att} is the rate at which nZVI attaches or is deposited on available collector sites (1/T), which could be described as [17]:

$$K_{\text{att}} = \frac{3(1-\theta_w)}{2d_{50}}\alpha\eta_o v_P, \tag{3}$$

where θ_w is the volumetric water content, d_{50} is the median collector grain size (L), α is sticking or removal efficiency, defined as the ratio of particles that attach to the collector to those that strike the collector, and η_o is the theoretical collision efficiency, defined as the ratio of particles striking the collector to those that approach the collector, which can be described by [25]:

$$\eta_o = \eta_D + \eta_I + \eta_G, \tag{4}$$

where η_D, η_I and η_G are diffusion, interception, and gravity terms, correspondingly.

In this study, the governing equations were solved using an analytical solution to Eq. (2), which could be described by [26]:

$$C(x,t) = \frac{m'}{4\pi n t\sqrt{D_x}} \exp\left[-\frac{((x-x_o)-vt)^2}{4D_x t} - \lambda t\right], \tag{5}$$

where m' is the injected contaminant mass per vertical unit (M/L), t is the time since the start of injection (T), n is the porosity, v is the seepage velocity, and λ is the decay coefficient (1/T).

When the partitioning of the contaminant is described with a linear isotherm, retardation of the front relative to the ground water flow could be expressed using a retardation factor, R:

$$R = \frac{v}{v_R} = 1 + \frac{\rho_b}{n}k_{\text{att}}, \tag{6}$$

where v is the velocity of the groundwater, v_R is the velocity of the $C/C_o = 0.5$ point on the concentration profile of the retarded constituent, and ρ_b is the bulk mass density of the porous medium. The determination of attachment coefficient, k_{att}, is essential to the evaluation of compound mobility in water.

When the coordinate system is aligned with the mean velocity vector, the longitudinal (D_L) hydrodynamic dispersion coefficient is related to the pore fluid velocity through the following equation:

$$D_L = \alpha_L |V| + D'_m, \tag{7}$$

where D'_m is the effective molecular diffusion coefficient of the solute in the porous medium, $|V|$ is the magnitude of the velocity vector, and α_L is the longitudinal component of the dispersivity tensor. α_L is considered the characteristic property of a region of a porous medium, and typically, is conveniently treated as independent of the pore fluid velocity and Péclet number [27].

To evaluate whether prepared S-nZVI suspension could be used for in-situ injection and delivery, its transport behavior was studied by conducting column experiments. The effects of some main parameters, including pore velocity and S-nZVI slurry concentration, were investigated. The pore velocities applied in the majority of column studies were much higher than those typically found in field scale approaches [19]. Results of laboratory tests at high water velocities may overestimate nZVI transmission in lower velocity, field scale applications, due to reduced nZVI attachment to porous media at higher velocities.

In this study, 25 loading conditions (trial) were applied, details of which are listed in Table 2. Prior to the main experiments by S-nZVI suspension, to compare the transport behavior of an ideal solute with iron nanosuspension through the used porous media, a series of tracer experiments using Rhodamine ($C_{28}H_{31}N_2O_3Cl$) were planned. Rhodamine is non-degrading, non-sobbing, rather inert, and non-reactive. In each trial, the stabilized nZVI slurry of one PV was pumped into the column. In addition, column effluents were sampled at certain time intervals and analyzed for concentrations of total and ferrous iron. All experiments were conducted in duplicate, and the results were averaged.

3. Results and discussion

3.1. Characteristics of S-nZVI

To characterize the stabilized iron nano particles, X-Ray powder Diffraction (XRD), Scanning Electron Microscopy (SEM), and Dynamic Light Scattering (DLS) were recorded, the results of which are shown in Figure 2. The starched nZVI particles displayed much less agglomeration than those prepared without a stabilizer, so that, while S-nZVI remained suspended in water for several hours, non-starched particles agglomerated and precipitated within minutes. XRD results, obtained by a D8 Advanced Bruker diffractometer, indicated the presence of Fe° (peaked at $2\theta = 42$, 67, 82), and Fe_2O_3 ($2\theta = 35$, 53). SEM analyses by a S4160 FE-SEM device denoted that the S-nZVI were present as discrete particles as opposed to dendritic flocs for non-starched nZVI. DLS was performed using a S-red Badge model ZEN1600. The mean particle size was estimated to be 78 nm with a standard deviation of 14 nm, which translated to a surface area of at least 15 m^2/g. This means that the synthesized particles were appropriate, in terms of size, for remediation purposes [12,13].

3.2. Column experiments

3.2.1. Tracer transmission

The breakthrough curves (BTC) of the tracer thorough glass beads and packed sand for the five velocities are shown as colored points in Figure 3. By assuming that the attachment coefficient, k_{att}, is equal to zero and the retardation factor, R, is equal to 1, other parameters were calculated using inverse fitting of the experimental data on the analytical solution offered in Eq. (5). The two fitted parameters were dispersion coefficient and pore velocity, and results of calibration are given in Figure 3(a) to (e). By assuming that longitudinal dispersivity coefficient, α_L, was independent of velocity, it was concluded that α_L was averagely equal to 2.6×10^{-3} m for glass beads media.

Further analysis of the breakthrough curves showed that, in the case of glass beads media, BTCs had a symmetrical shape and no tailing, thus, indicating that the physical non-equilibrium processes, such as rate-limited mass transfer into regions of immobile

Table 2. Details of column experiments.

Trial no	Porous material	Injected suspension	Pore velocity m/d				
1 to 5	Transparent media*	Tracer	9	21	27	44	74
6 to 10		0.3 g/L S-nZVI	9	21	27	44	74
11 to 15		3 g/L S-nZVI	9	21	27	44	74
16 to 20	Packed sand	Tracer	7	19	32	55	85
21 to 25		3 g/L S-nZVI	7	19	32	55	85

* Glass-beads porous media is called here transparent media.

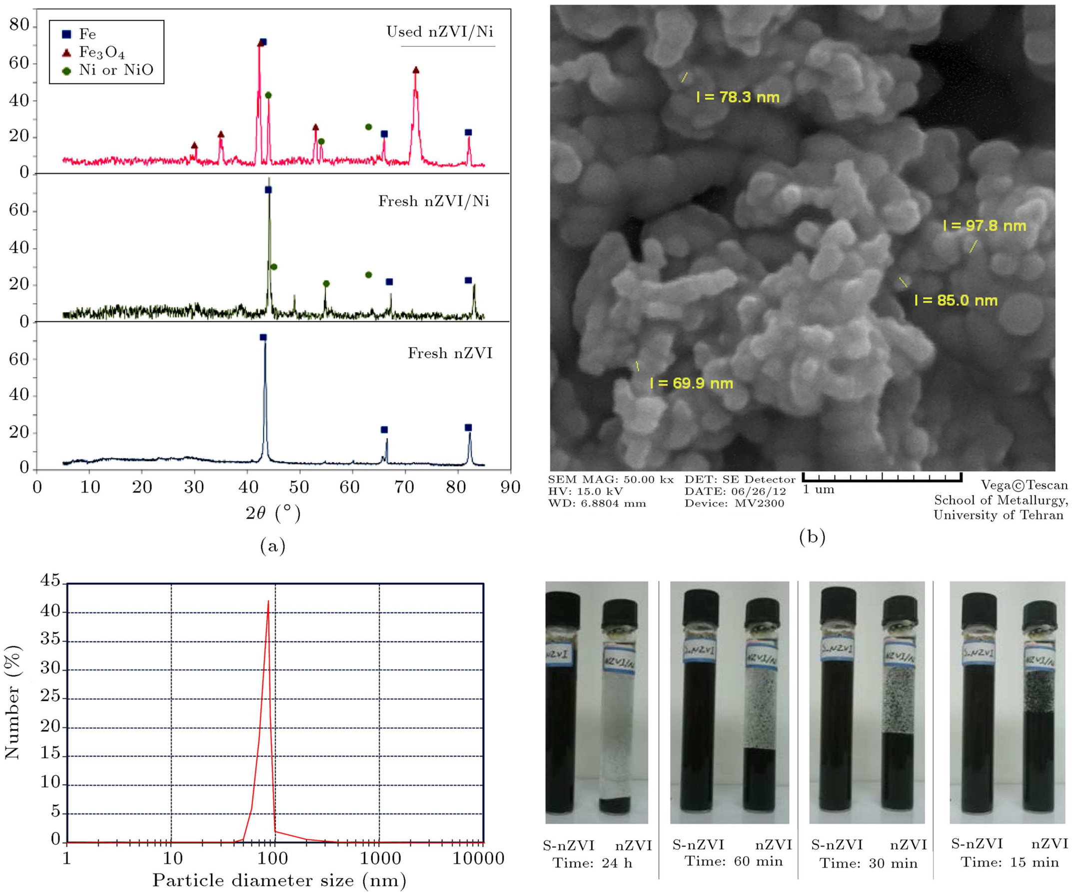

(a) (b) (c) (d)

Figure 2. Characteristic of synthesized S-nZVI: (a) XRD diagram; (b) SEM image; (c) DLS results; and (d) stability status.

water and preferential flow paths, were not present during transport through porous media.

In the case of sand media, BTCs had a rather non-symmetrical shape. Thus, $R \neq 1$ and fitted parameters were k_{att}, D, and v, and the results of calibration are given in Figure 3(f) to (j). Similarly, dispersivity coefficients, α_L, for packed sand media, are obtained as 2.2×10^{-3} m.

3.2.2. S-nZVI transmission

It is known that the effective velocity of a particle in a porous medium is rather more than that observed for water and solutes. However, under some conditions, the difference could be ignored and the effective velocity of a particle could be approximated with the values obtained from tracer tests [18]. For the particle size and flow rates used in this work, the average pore diameter was 5×10^{-4} m and the ratio of colloid to water flow rate was less than 0.5%. These values were small enough to support the use of parameters obtained from tracer tests, such as dispersivity coefficients, to assess S-nZVI mobility in porous media. The results of S-nZVI/Ni injection in column tests could be found in the following parts. But, as a general rule, experimental and model curves were in full compliance, both for inverse-simulated tests and for the others. The calculated R-squared values, R^2, had a range of 0.7 to 1, and the P-values had a significance level of 75% under most circumstances, except for a few cases of BTCs, when nZVI concentration was equal to 3 g/l and pore velocity less than 15 m/s. A slightly more pronounced discrepancy was noticed for the higher nanoparticle concentrations, but, overall, the quantitative and qualitative agreement was satisfactory.

a. Glass beads media

The observed BTCs of nanoparticles in a transparent column, as a function of time, in different experimental conditions of pore water velocities (v = 9, 21, 27, 44 and 74 m/d) and injected concentrations (C_o = 0.3 and 3 g/l), are presented in Figure 4 by colored points. Parameters were calculated by using the inverse fitting of experimental data on the analytical solution. As indicated in Figure 4, both pore velocity and slurry concentration had a significant impact on S-nZVI transmission in porous media. Using 0.3 g/l nZVI concentration, the retardation factor at 9 m/d pore velocity was about 1.3, but was nearly 1.1 when

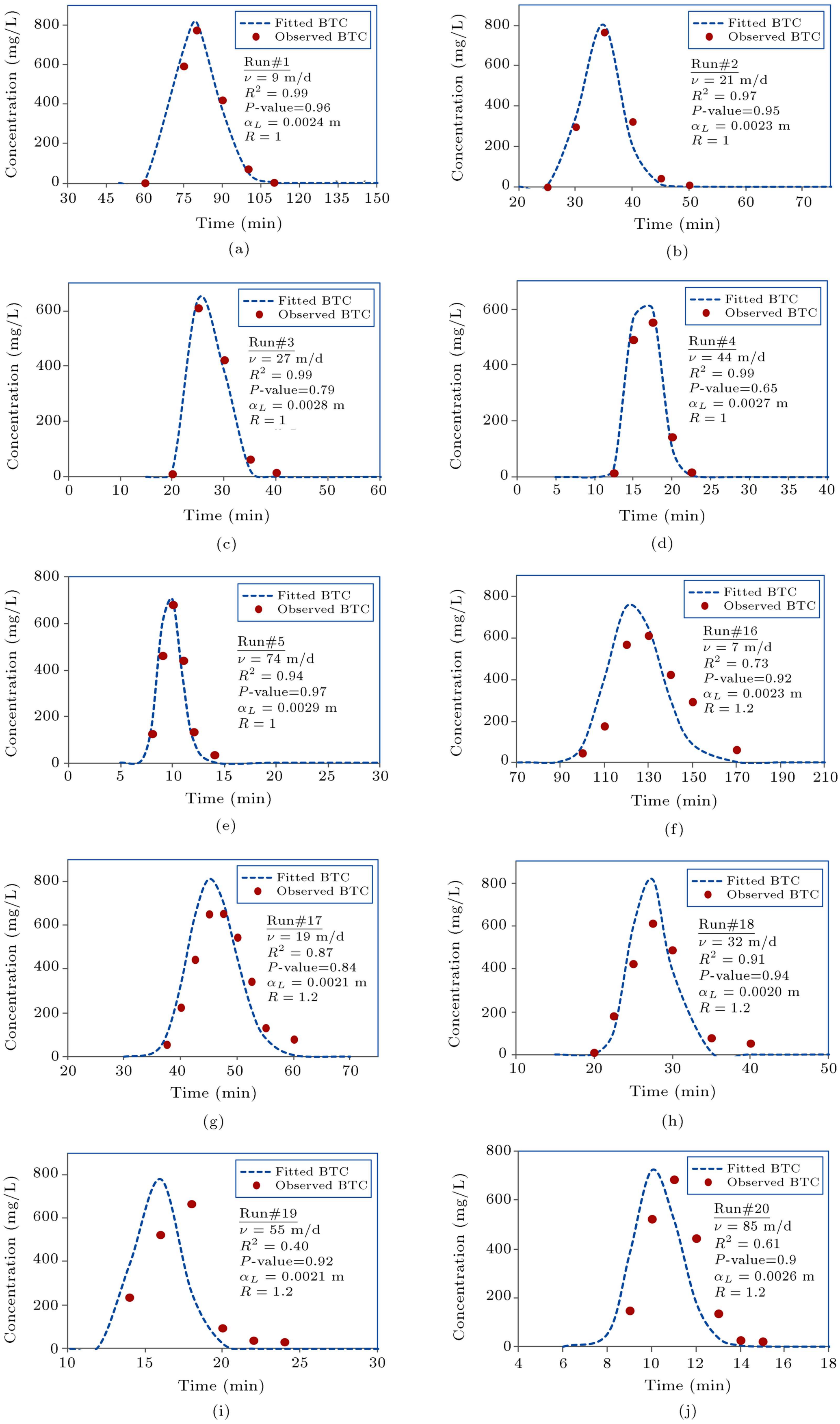

Figure 3. Tracer breakthrough cures in transparent column experiments.

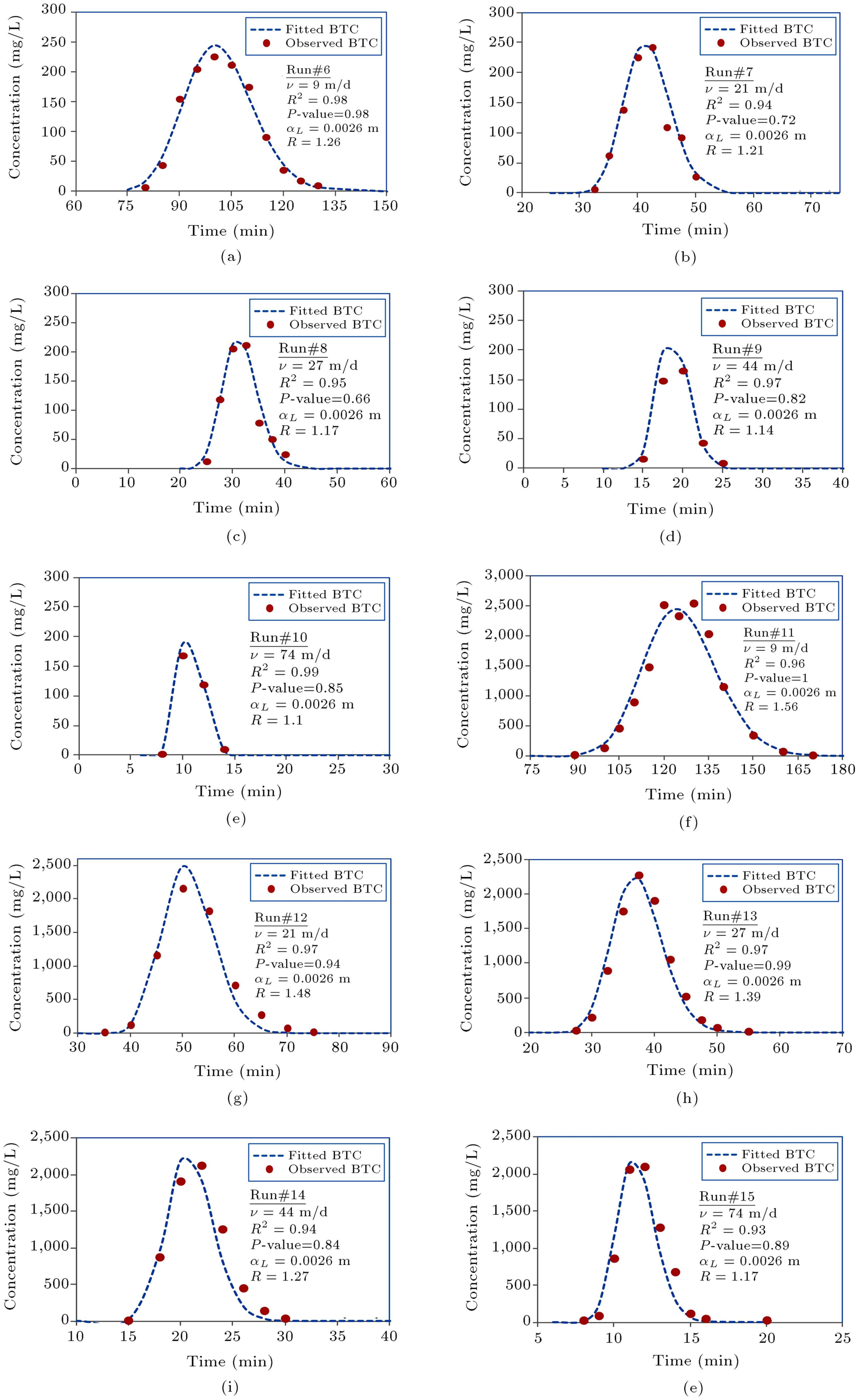

(a) (b)

(c) (d)

(e) (f)

(g) (h)

(i) (e)

Figure 4. S-nZVI breakthrough cures in transparent column experiments.

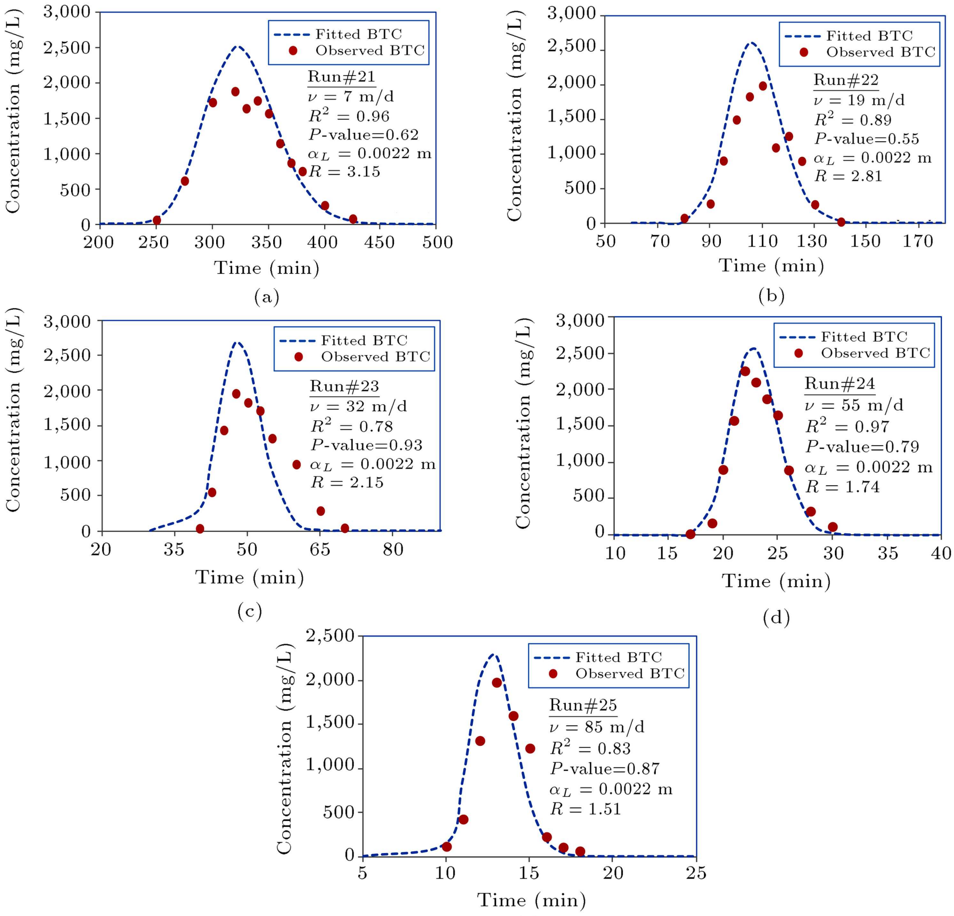

(a) (b) (c) (d) (e)

Figure 5. S-nZVI breakthrough cures in sand column experiments.

the pore water velocity was over 70 m/d. In the same cases, using 3 g/l nZVI slurry, the retardation factor, at 9 m/d pore velocity, was about 1.6, but was nearly 1.2 when the pore water velocity was over 70 m/d. A retardation factor of 1.6 implies that the nZVI plume moves 1.6 times slower than the pore water velocity. These phenomena could be attributed to an increase in drug forces and shear stress resulting from the increase in pore water velocities, where decline clogging and the detachment phenomena occurred. Further analysis of the breakthrough curves showed that release during flushing increased, mainly, by increasing the injected concentration, C_o, while flow rate had a minor impact. For low concentration, C_o = 0.3 g/l, the decline of the BTCs at the beginning of flushing was abrupt, regardless of the flow rate. For high concentration, C_o = 3 g/l, a slightly retarded decline of breakthrough concentration was observed, suggesting that a fraction of the deposited particles were released. It seems that this behavior is associated with the value of C_o, rather than to the pore water velocity, as the flow rate affected the position of the BTC peak, but did not have a relevant influence on its height and shape.

b. Packed sand media

Using colored circles, Figure 5 illustrates the obtained breakthrough curves of S-nZVI in a sand column as a function of time. Experimental conditions were adjusted as pore water velocities of 7, 19, 32, 55 and 85 m/d, injected concentration of $C_o = 3$ g/l, and assuming $\alpha_L = 2.2 \times 10^{-3}$ m. As shown, the breakthrough curves were unsymmetrical, which implied that attachment and detachment phenomena occurred. Using inverse fitting of the experimental data on the analytical solution, the retardation factors for the above mentioned pore velocities were indicated as 3.15, 2.81, 2.15, 1.74 and 1.51, correspondingly. As expected, S-nZVI/Ni retardation decreased when pore velocity increased. This is consistent with the literature for colloid transport in general, and for iron-based nano-particles in particular [28]. A comparison between Figures 4 and 5 suggests that lower S-nZVI concentration in the effluent compared to the feed could be exclusively attributed to the retention of nZVI in the sand medium.

In the present study, colloid filtration and column experiment theory was used to estimate the effective and maximum travel distance of nZVI for application in the field remediation projects. Therefore, it is necessary that ZVI slurry and porous media used during column tests have similar properties with the soil in the field. Several researchers have previously described the mobility of iron nano-particles through sand with the help of the colloid filtration theory, as a process controlled by a first-order kinetics mechanism [18]. An additional term $(-k_r C)$ was introduced in the CFT equation to account for the removal of nZVI, as shown in Eq. (5). The first-order rate kinetic constant, k_r, could be calculated from the experimental column data, according to following equation [18]:

$$K_r = -(v/L)\ln(C_e/C_o), \tag{8}$$

where k_r is a first-order kinetics rate constant for nZVI retention, L is the length of the column, C_o is the initial concentration of nZVI, and C_e is the steady state concentration of nZVI in the effluent. Eq. (8) could be rearranged, as shown in Eq. (9), to calculate the effective travel distance, R_{eff}, needed for nZVI concentration to be reduced to 10% of the initial concentration:

$$R_{\text{eff}} = -(v/K_r)\ln(C_{\text{effective}}/C_o). \tag{9}$$

R_{eff} was calculated for several values of pore velocity, ranging between 1 and 80 m/d and initial nZVI concentration; the results appear in Figure 6. Regarding the impact of pore water velocity on S-nZVI transport, Figure 6 shows that increasing the pore water velocity decreases the tailing phenomenon and enhances mobility. This is due to the fact that increasing pore water velocity will increase drag momentum and enhance the detachment of nZVIs [19]. It is noted that in low pore velocities, typical of groundwater flow velocities, the nZVI travel distance was limited to the range of 0.1 to 0.5 m. At higher velocities, which could be the case during the injection of nZVI suspension in the field for remediation purposes, travel distance may reach a range of 1 to 10 m. For instance, at pore velocities of 25 and 50 m/d, the calculated travel distances reach 1.5 and 5 m, respectively.

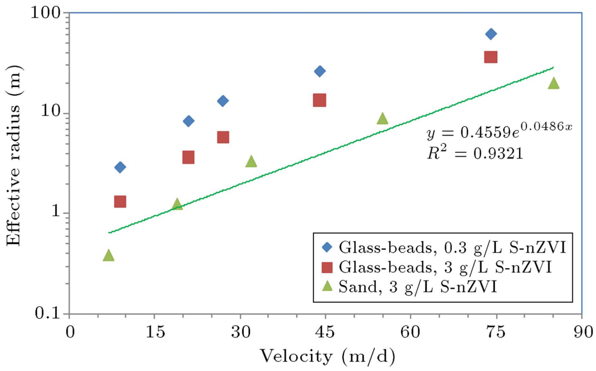

Figure 6. Effective traveling distance of S-nZVI in column experiments.

He et al. [21] studied the penetrability of CMC stabilized nZVI in sand columns, using a rather diluted suspension. From their results, it could be calculated that, at a Darcy velocity of 1 m/d, nanoparticles would travel a maximum distance of almost 1.1 m, which is approximately 3 times longer compared to the travel distance of S-nZVI/Ni produced in the current study, at the same Darcy velocity. However, mobility results are not directly comparable, because of the difference in modeling conditions and nZVI slurry concentrations.

4. Conclusions

In this study, starched nZVI, with an average particle size of 74 nm, was synthesized and applied in column experiments. The influence of pore velocity, porous media, grain size and type, and injection suspension concentration on S-nZVI transfer was investigated. The experimental approach was designed to be representative of conditions expected at field scale remediation projects. As expected, the calculations showed that at low pore water velocities, typical of natural groundwater flow rates (< 10 m/d), S-nZVI remained within a short distance from their initial position (< 0.5 m). In addition, at higher velocities, which may prevail during the in-situ injection process, the nanoparticles were able to reach a longer distance; e.g. for a pore velocity of 50 m/d, the travel distance was in the order of 5 m. It was also determined that the type of porous material and nZVI concentration were the main parameters in controlling the transport properties of S-nZVI. Furthermore, one may conclude that bench scale test conditions should replicate, as closely as possible, intended field scale conditions, with respect to pore water velocity, grain type and size, S-nZVI slurry concentration, and injection duration.

List of abbreviations

nZVI	nano Zero Valent Iron particles
S-nZVI	Stabilized nano Zero Valent Iron particles
PRB	Permeable Reactive Barrier
XRD	X-Ray powder Diffraction
SEM	Scanning Electron Microscopy
DLS	Dynamic Light Scattering
BTC	Breakthrough Curve

Acknowledgments

This work was supported by the Institute of Biotechnology and the Environment (IBE) at Sharif University of Technology, Tehran, Iran.

References

1. Savage N., D.M.S. "Nanomaterials and water purification: opportunities and challenges", *J. Nanoparticle Res.*, **7**(4-5), pp. 331-342 (2005).
2. Li, L., Benson, C.H. and Lawson, E.M. "Modeling porosity reductions caused by mineral fouling in continuous-wall permeable reactive barriers", *Journal of Contaminant Hydrology*, **83**, pp. 89-121 (2006).
3. Zhang, X., Lin, S., Lu, X.-Q. and Chen, Z.-l. "Removal of Pb(II) from water using synthesized kaolin supported nanoscale zero-valent iron", *Chemical Engineering Journal*, **163**, pp. 243-248 (2010).
4. Cundy, A.B., Hopkinson, L. and Whitby, R.L.D. "Use of iron-based technologies in contaminated land and groundwater remediation: A review", *Science of The Total Environment*, **400**, pp. 42-51 (2008).
5. Rangsivek, R. and Jekel, M.R. "Removal of dissolved metals by zero-valent iron (ZVI): Kinetics, equilibria, processes and implications for stormwater runoff treatment", *Water Research*, **39**, pp. 4153-4163 (2005).
6. Fadaei, M.R., Vossoughi, M. and Shamsai, A. "In-situ nitrate remediation using nano iron/nickel particles", *Environment Protection Engineering*, **40**, pp. 75-86 (2014).
7. Yang, G.C.C. and Lee, H.-L. "Chemical reduction of nitrate by nanosized iron: kinetics and pathways", *Water Research*, **39**, pp. 884-894 (2005).
8. Zhang, X., Deng, B., Guo, J., Wang, Y. and Lan, Y. "Ligand-assisted degradation of carbon tetrachloride by microscale zero-valent iron", *Journal of Environmental Management*, **92**, pp. 1328-1333 (2011).
9. Fadaei, M.R., Shamsai, A. and Vossughi, M. "In-situ Pb^{2+} remediation using nano iron particles", *Journal of Environmental Health Science & Engineering*, **13**(1) (2015). DOI 10.1186/s40201-015-0157-3
10. Kim, K.-R., Lee, B.-T. and Kim, K.-W. "Arsenic stabilization in mine tailings using nano-sized magnetite and zero-valent iron with the enhancement of mobility by surface coating", *Journal of Geochemical Exploration*, **113**, pp. 124-129 (2012).
11. Fagerlund, F., Illangasekare, T.H., Phenrat, T., Kim, H.J. and Lowry, G.V. "PCE dissolution and simultaneous dechlorination by nanoscale zero-valent iron particles in a DNAPL source zone", *Journal of Contaminant Hydrology*, **131**, pp. 9-28 (2012).
12. Noubactep, C. "A critical review on the mechanism of contaminant removal in Fe^{o}-H_2O systems", *Environ. Technol.*, **29**, pp. 909-920 (2008).
13. O'Carroll, D., Sleep, B., Krol, M., Boparai, H. and Kocur, C. "Nanoscale zero-valent iron and bimetallic particles for contaminated site remediation", *Adv. Water Resour.*, **51**, pp. 104-122 (2013).
14. Zhang, W.X. "Nanoscale iron particles for environmental remediation: an overview", *J. Nanoparticle Res.*, **5**(3-4), pp. 323-332 (2003).
15. Wang, D.J. "Transport behavior of humic acid-modified nanohydroxyapatite in saturated packed column: effects of Cu, ionic strength, and ionic composition", *J. Colloid Interface Sci.*, **360**(2), pp. 398-407 (2011).
16. Saleh, N., Kim, H.J., Phenrat, T., Krzystof, M., Tilton, R. and Lowry, G. "Ionic strength and composition affect the mobility of surface-modified feo", *Nanoparticles in Water-Saturated Sand Columns. Environ. Sci. Technol.*, **42**, pp. 3349-3355 (2008).
17. Kocur, C.M., O'Carroll, D.M. and Sleep, B.E. "Impact of nZVI stability on mobility in porous media", *Journal of Contaminant Hydrology*, **145**, pp. 17-25 (2013).
18. Hosseini, S.M. and Tosco, T. "Transport and retention of high concentrated nano-Fe/Cu particles through highly flow-rated packed sand column", *Water Research*, **47**, pp. 326-338 (2013).
19. Fagerlund, H.J., Illangasekare, F., Tilton, T. and Lowry, G.V. "Particle size distribution, concentration, and magnetic attraction affect transport of polymer-modified Feo nanoparticles in sand columns", *Environmental Science & Technology*, **43**, pp. 5079-5085 (2009).
20. Phenrat, T., Saleh, N., Sirk, K., Kim, H.J., Tilton, R.D. and Lowry, G.V. "Stabilization of aqueous nanoscale zero-valent iron dispersions by anionic polyelectrolytes: adsorbed anionic polyelectrolyte layer properties and their effect on aggregation and sedimentation", *J. Nanopart Res.*, **10**, pp. 795-814 (2008).
21. He, F. and Zhao, D. "Preparation and characterization of a new class of starch-stabilized bimetallic nanoparticles for degradation of chlorinated hydrocarbons in water", *Environ. Sci. Technol.*, **39**, pp. 3314-3320 (2005).
22. Lee, C., Jee, Y.K., Won, I.L., Nelson, K.L., Yoon, J. and Sedlak, D.L. "Bactericidal effect of zero-valent iron nanoparticles on Escherichia coli", *Environmental Science and Technology*, **42**, pp. 4927-4933 (2008).
23. Kanel, S.R., Neppolian, B., Choi, H. and Yang, J.W. "Heterogeneous catalytic oxidation of phenanthrene by hydrogen peroxide in soil slurry: Kinetics, mechanism, and implication", *Soil and Sediment Contamination*, **12**, pp. 101-117 (2003).
24. Yao, K.M., Habibian, M.T. and O'Melia., C.R. "Water and waste-water filtration: Concepts and applications", *Environ. Sci. Technol.*, **5**, pp. 1105-1112 (1971).
25. Tufenkji, N. and Elimelech, M. "Correlation equation for predicting single-collector efficiency in physiochemical filtration in saturated porous media", *Environ. Sci. Technol.*, **38**, pp. 529-536 (2004).
26. Bedient, P.B., Rifai, H. S. and Newell, C.J., *Groundwater Contaminant*, Prentice Hall PTR, pp. 151-189 (1999).
27. Gaganis, P., Kjeldsen, P. and Burganos, V.N. "Modeling natural attenuation of multicomponent fuel mixtures in the vadose zone: Use of field data and evaluation of biodegradation effects", *Vadose Zone J.*, **3**(4), pp. 1262-1275 (2004).

28. Tiziana, T., Julian, B., Rainer, M. and Rajandrea, S. “Transport of ferrihydrite nanoparticles in saturated porous media, role of ionic strength and flow rate”, *Environmental Science & Technology*, http://dx.doi.org/10.1021/es202643c (2012).

Biographies

Mohamad Reza Fadaei Tehrani received his BS degree in Civil Engineering and MS degree in Hydraulic Structures Engineering, in 2003 and 2005, respectively, from Sharif University of Technology, Tehran, Iran, where he is currently a PhD degree candidate in the Department of Civil Engineering. His research interests include water and wastewater treatment, groundwater remediation, image processing and nano-particles technology.

Abolfazl Shamsai received his PhD degree from the Department of Civil Engineering at the University of California, Davis, USA, in 1981, and then completed post-doctoral studies at the University of California, Berkeley, USA, from 1988 to 1990. Dr. Shamsai is currently Professor in the Civil Engineering Department at Sharif University of Technology (SUT), Tehran, Iran, where he has taught multiple courses in the fields of water and dam engineering, and been advisor to many MS and PhD students. In 1995, Dr. Shamsai was presented with the national exemplary professor award by SUT. Since 1971, he has 415 publications, including 17 books, 160 conference papers, and 128 journal papers, published in Iranian and foreign journals.

Manouchehr Vossoughi received a BS degree in Chemical Engineering from Sharif University of Technology (SUT), Tehran, Iran, in 1974, and MS and PhD degrees in Biotechnology from the Department of Chemical Engineering at the University of Toulouse, France, in 1979 and 1983. Dr. Vossoughi is currently faculty member and Professor in Bio- and Nano-Technology in the Department of Chemical Engineering and Petroleum at Sharif University of Technology, Tehran, Iran. His research interests include microbial enhanced oil recovery, new surfactants in petroleum engineering and application of nano technology in oil production enhancement.